U.R.S.I. FRANCE JS 20

FUTURE NETWORKS: 5G AND BEYOND

Performances en puissance et délai pour des communications optiques sans fil dans un cockpit

Power and Delay performance of Optical Wireless Communication inside Aircraft Cockpit

Steve Joumessi-Demeffo[1], Stephanie Sahuguede[1], Anne Julien-Vergonjanne[1], Pierre Combeau[2], Lilian Aveneau[2], Hervé Boeglen[2], Damien Sauveron[1]

[1] University of Limoges, CNRS, XLIM UMR 7252, F-87000 Limoges, France, {steve.joumessi-demeffo ; stephanie.sahuguede ; anne.julien-vergonjanne; damien.sauveron}@unilim.fr

[2] University of Poitiers, CNRS, XLIM UMR 7252, F-86000 Poitiers, France {pierre.combeau ; lilian.aveneau herve.boeglen}@univ-poitiers.fr

Keywords/Mots clés : Li-Fi, optical wireless communication, channel modeling, channel access control
Li-Fi, communications optiques sans fil, modélisation du canal, méthodes d'accès

Abstract/Résumé

This work investigates optical wireless links between four pilot headsets and access point inside aircraft cockpit for audio and physiological data transmission. We determine the impact of optical wireless channel on DCF (Distributed Coordination Function) control mechanism performance. The results show the trade-offs between emitted optical power and communication delay.

Ce travail présente l'étude de liaisons optiques sans fil entre les casques des pilotes et le point d'accès à l'intérieur d'un cockpit d'avion pour la transmission de données audio et physiologiques. Nous déterminons l'impact du canal optique sans fil sur les performances du mécanisme d'accès au canal DCF (Distributed Coordination Function). Les résultats montrent les compromis entre la puissance optique émise et le délai de communication.

1 Introduction

The aeronautical industry is constantly seeking to introduce new technologies to improve aircraft performance and their ecological impact, but also to increase the safety and comfort of crews and passengers. Thus, the use of wireless communication technologies to replace aircraft cables can help reduce weight and therefore fuel consumption and CO2 emissions but can also improve crew efficiency [1]. Indeed, the majority of pilots are now looking for high-performance wireless headsets because they contribute to comfort, especially for long-haul flights, which require the pilot constantly wearing his headset for long hours. Wired headsets are well known to cause pain and reduce mobility. This contributes to increase pilot stress, which can be critical, especially for operations where the safety margin is already low (for example, take-off or landing). Wireless connectivity in the cockpit therefore makes perfect sense to support pilot operations and decision-making aimed at improving the performance and efficiency of the crew on duty, reducing the workload and the risk of human error. The wireless communications currently available in the cockpit are Wi-Fi and Bluetooth. Although effective, these solutions suffer from some drawbacks. Due to radio waves propagation, one problem is that the signal can be scrambled or listened to [2]. In addition, radiofrequencies (RF) are sensitive to electromagnetic interference. These issues render RF technologies unsuitable for such a sensible environment as the cockpit where safety and security are paramount.

Optical wireless communication (OWC) is today the most promising candidate capable of overcoming these disadvantages because it provides a secure mode of communication [3-6]. Indeed, optical waves cannot pass through walls or opaque objects. Thus, unlike RF communications, it is very difficult to hack the link and take control. In addition, the use of optical wavelengths guarantees the absence of electromagnetic interference with other electronic devices. However, these advantages can also constitute limitations because the range is limited and the performances are very sensitive to blockages. Thus, one of the main challenges in airplanes context relies on ensuring coverage, requiring a thorough analysis of the communication channel. Several projects have studied the use of OWC technology in aircraft, generally for applications and services relating to passengers in the cabin [7-11]. For example, the scenarios studied concern entertainment [7], video broadcasting [8], communications between passengers [9], and even medical surveillance of travelers [10]. In [11] the infrared optical wireless path loss inside an aircraft cabin is estimated. However, the optical channel in the cockpit has not yet been much studied, this environment having a particular geometric complexity and expected connection blockages due to the pilot's movements. In [12], we have studied for the first time the OWC channel between optical transceivers included on two pilot headsets and an access point located at the cockpit ceiling. This work was based on a Monte Carlo ray-

tracing methodology, from the 3D representation of an aircraft cockpit including pilot and copilot body models and head movements. Based on the channel analysis we have determined the channel path losses corresponding to 100% link reliability. Here, we have first extended our study presented in [12] by considering four pilots inside the cockpit whose heads and bodies can move. Based on channel analysis, our aim is to investigate network performance for audio transmissions between pilot headsets and one access point located in the cockpit. As the brightness in the cockpit must be greatly reduced during critical flight phases, the visible band is not appropriate. Therefore, optical wavelengths in the infrared (IR) range are used. Moreover, one main specification for audio headset is to guarantee sufficient autonomy to ensure long-haul flights. In order to satisfy this constraint, typical single carrier modulation schemes for OWC systems which are easy to implement and power efficient are considered [13, 14]. In addition, these modulation schemes are known to be suitable for low-medium data rate applications such as audio transmissions. Furthermore, considering that pilots can use the headset in other environments than the cockpit, we are interested in the IEEE 802.11 channel access standard such as carrier-sense multiple access with collision avoidance (CSMA/CA). Indeed, currently there are standardization efforts on the commercial development of OWC technology, in particular Li-Fi [15], which aim at interoperability with Wi-Fi standards. In this work, we will consider the DCF (Distributed Coordination Function) algorithm with RTS/CTS (Request To Send /Clear to Send) method [16]. One main impact of channel access method is on delay between the acoustic signal and the audio management unit of the aircraft, which can decrease as data rate increases, considering a given data packet size. On the other hand, we have also to consider limitations on data rate to achieve a given performance in terms of Bit Error Rate (BER) linked to autonomy and IR eye safety constraints.

Consequently, the main contribution of this paper is to highlight the trade-offs between minimal optical emitted power needed to attempt a given BER for typical OWC modulation schemes [13] and successful communication delay, considering a network based on IEEE802.11 channel access mechanism with four optical wireless pilot headsets and one access point inside the cockpit. The remainder of the paper is organized as follows. Section 2 presents the description of cockpit environment including crew presence and the extended channel analysis. We then introduce in section 3 the used modulation performance related to optical emitted power and the definition of communication delay regarding DCF method. Section 4 shows the results and discussions on trade-offs before conclusion.

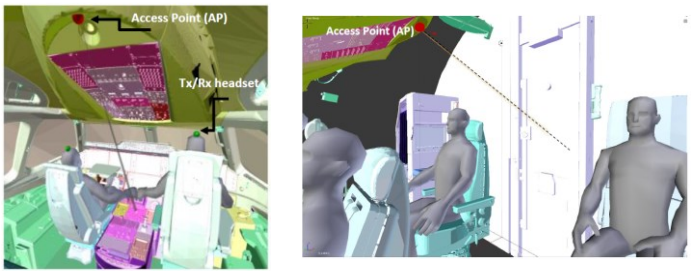

Figure 1: AIRBUS A350 cockpit, AP and pilot/co-pilots position

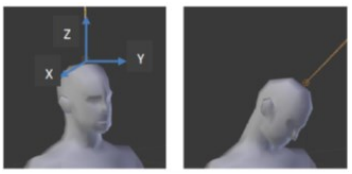

Figure 2 : Tx/Rx headset orientation on the head top

2 Cockpit environment and channel model

2.1 Environment description

The studied environment is the cockpit of an AIRBUS A350 aircraft. In this environment, we are focusing on a scenario using optical wireless links to ensure the connectivity of the headsets worn by the crew (pilot, co-pilot, third and four occupants). We consider the IR bidirectional link between the transceivers (Tx/Rx) integrated on the headset and those located on the cockpit ceiling at the access point (AP). There are two pairs of transceivers on AP. The first one is situated at about 1m from the top of the pilot and co-pilot heads (see Fig. 1, with orientation in grey line). The second pair is at the same location but with orientation towards the cockpit door between the two third and four occupant at the cockpit rear (Fig. 1 with orientation in dotted line). In addition, note in Fig.1, that pilot and co-pilot seats have different settings corresponding to the two extreme possible positions. The pilot is the farthest from the control panel (the face is at 60 cm) at the lowest height (the top of the head is 40 cm under the ceiling and 1.17 m above the floor). The co-pilot is the closest to the control panel (the face is at 45 cm) at the highest height (the top of the head is 15 cm under the ceiling, 1.30 m above the floor). For the headset, we have considered one location of Tx/Rx on the top of pilot head. They are oriented parallel to user spine (see Fig. 2), but it can randomly change according pilot movements, inducing link attenuation or blockages.

2.2 Channel model

To determine the channel impulse response for uplink between the headset and the AP, the reverse in downlink,

we adopted a modeling approach based on a stochastic Monte Carlo method, associated with the ray-tracing algorithm [12, 17]. This methodology allows determining the received power for Line-Of-Sight (LOS) and non-LOS (NLOS) paths, i.e. reflected paths over all the elements inside the cockpit. Actually, because of random movements of pilot, the LOS link condition cannot always be fulfilled. Thus, we have developed a detailed 3D geometric model of the cockpit (illustrated in Fig.1) generated from a CAO file provided by AIRBUS, and then imported into our software [12]. In addition, we have included the pilots' bodies, fully articulated and animated using the Blender software [18]. The mobility scenario we have studied considers that a pilot first looks ahead and then turns his/her head to the left, then tilts it forward, and then turns it to the right before returning it to its initial position. This is illustrated in Fig.3 (a). In addition, we have also simulated the case where a pilot has to lean to the ground to pick up a fallen object (see Fig.3 (b)).

(a) *(b)*

Figure 3: (a) Head movement (b) Body movement

Each of these discretized movements induces different IR links according to the orientation changes of the headset transceivers. So this corresponds to a set of impulse responses *h(t).* One of the main parameters characterizing the optical channel is the DC gain H_0, which is related to *h(t)* by [13] :

$$H(0) = \int_{-\infty}^{+\infty} h(t)dt = H_0 \qquad (1)$$

Other features are time dispersion parameters related to *h(t)* length and mean delay spreading. Here, all the surfaces in the scene and the bodies are considered as perfectly diffuse and are consequently modeled using a Lambertian Bidirectionnal Reflectance Distribution Function (BRDF) [17]. The reflection coefficients are set to 0.5, which is the mean value between absorbent and perfectly reflective material [12]. The receivers on headset and AP are generic IR photodiodes with Field-Of-View of 60° and surface detection of 7mm². Moreover, the optimal half-power angles of emitters on headset, respectively on AP, are of 60°, respectively 40°, as established in [12]. With these parameters, we have verified that the temporal dispersion induced by the reflected paths can be ignored for data rate lower than 20 Mbps. In the following, we only focus on the DC gain and neglect inter-symbol interference.

	uplink Head movement	uplink Body movement	downlink Head movement	downlink Body movement
Pilot	-70.3	-69.4	-69.7	-67.2
Co-pilot	-72.1	-71.9	-71.2	-70.1
Pilot rear	-66.5	-67.9	-65.5	-68
Copilot rear	-61.1	**-72.2**	-52.7	**-74**

Table 1: Minimum DC gain (dB)

To investigate the performance of the network constituted of the 4 headsets and the access point, we consider the case where the gain value is the most reliable among all the possible values linked to the movements of the pilots. This corresponds to the lowest gain values obtained in each case. Table 1 reports the minimum H_0 values in dB. We first observe that the head movements are the most penalizing for the headsets worn by the pilot and co-pilot while for the occupants in the rear it is the body movements. In addition, for pilot and co-pilot headsets the lowest DC gains are obtained in uplink whereas this is for the downlink for rear pilot and rear co-pilot. Finally, considering all the cases, the worst corresponds to the bidirectional link with the rear co-pilot headset (in bold in Table 1).

3 Emitted power and communication delay

In this part, we first consider the emitted power required to attempt a given BER for classical optical modulation schemes. Then, to determine the delay, we describe the multi-user medium access control mechanism that is DCF algorithm with RTS/CTS method. As the delay diminishes with the data rate, while the required power increases, our objective is to analyze the compromise for OWC-based audio transmission inside aircraft cockpit.

3.1 Emitted power

The channel analysis has been performed in previous section in term of optical DC gain H_0. For a fixed average emitted power P_t, the SNR is expressed as [13]:

$$SNR = \frac{H_0^2 P_t^2 R^2}{2qI_B.B} \quad (2)$$

Where R is the photodiode responsivity set to 1 A/W in the following, q is the electron quantum charge and B the bandwidth of the modulated signal equal to the data rate R_b. For indoor environments, a classical assumption is to consider the noise as Additive White Gaussian Noise (AWGN) with power linked to induced ambient current I_B whose typical values is 200 µA for I_B [19].
Moreover, BER performance of typical modulation schemes depends of SNR. OOK (On-Off Keying) modulation is the basic modulation for OWC communication systems due to its simple implementation. The BER_{OOK} is expressed as follows:

$$BER_{OOK} = \frac{1}{2} erfc\left(\sqrt{\frac{SNR}{2}}\right) \quad (3)$$

As the use-case of audio headset needs power autonomy, we also study a power-efficient modulation scheme, standardized for OWC, which is L-level PPM (Pulse Position Modulation). L-PPM maps M bits of binary data into a single pulse placed at one of the $L=2^M$ possible positions or slots. It has been shown [6], that the BER_{L-PPM} is obtained from:

$$\begin{cases} BER_{L-PPM} = \frac{\frac{L}{2}}{L-1} P_{sye-PPM} \\ P_{sye-PPM} = 1 - (1 - P_{sle-PPM})^L \\ P_{sle-PPM} = \frac{1}{2} erfc\left(\sqrt{\frac{LM\ SNR}{4}}\right) \end{cases} \quad (4)$$

Where $P_{sye-PPM}$ is the symbol error rate and $P_{sle-PPM}$, the slot error probability.
By exploiting the expressions (3) and (4) for OOK and L-PPM, we can determine the targeted values of SNR for a given BER performance. Then, using the values of Table 1 for DC-gain and equation (2) it is possible to obtain the requested P_t value for the studied system according the data rate R_b.

3.2 Communication delay

To ensure multi-user communication, we propose an approach based on 802.11 medium access control mechanism. We are interested in the DCF basic method, which is used for 802.11 devices [16], and investigated for Li-Fi [20].The DCF method is known as Carrier Sense Multiple Access with Collision Avoidance (CSMA/CA) mechanism. With the basic DCF, if the channel is free for the transmitters, each one randomly chooses a waiting time called backoff contention windows (CW), which is in the interval [CWmin, CWmax].The waiting time is thus expressed in number of slot time (N_s) defined by the standard (see Table 2). As long as the channel is detected idle for a slot time, the backoff is decreased by one. The communication begins when it is to zero if the channel is free. When the channel is busy, the timer counter is blocked and resumes when the channel is inactive again for at least one slot time. One strong limitation of DCF arises from the obligation to send a request to the physical layer to know if the channel is free. Indeed, the node has to be able to listen the channel. This is the well-known issue of hidden nodes, which can be relaxed by the use of RTS/CTS mechanism which is optional in WLANs but mandatory in Li-Fi networks [20]. The compromise is additional exchanges introducing transmission overhead. The scenario of the RTS/CTS process is illustrated in Fig.4. The sending node uses an RTS frame for the receiver node after a distributed inter-frame space (DIFS) waiting time. The other nodes present in its coverage area receive this frame and initialize their NAV (Vector Allocator Network) counter. During NAV time, they know that they cannot transmit frames at the risk of causing collisions. The receiving node responds after a short inter-frame space (SIFS) with a CTS frame. Other nodes present in its CTS coverage area initialize their NAV. If the listening of the channel goes well, the sending node waits for the SIFS duration and sends a data frame. An ACK acknowledgment is received after a short SIFS period if the transmission is correct. Table 2 contains the specifications for the DCF method with RTS/CTS that we consider, where R_b is the PHY data rate. The values of RTS , CTS ,ACK and data take into account the PHY overhead. The metrics usually used to analyse the network performance are throughput

and delay. We use an analytical approach to evaluate these criteria, based on the Bianchi's [21] model and its extension proposed in [22]. In these models, the slot time duration indicates the time during which a node needs to detect the transmission of other nodes [22].

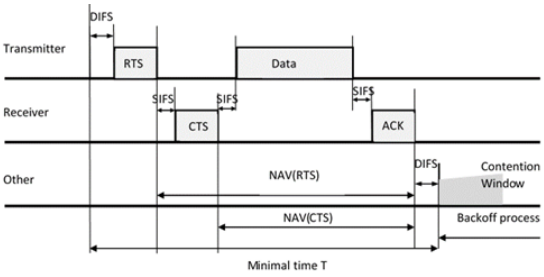

Figure 4: Principle of DCF mechanism with RTS/CTS

Attribute	Values
RTS (s)	288(bits)/ R_b
CTS (s)	240(bits)/ R_b
ACK (s)	240(bits)/ R_b
Data (s)	(MPDU+128) (bits)/ R_b
Media access control Protocol Data UnitMPDU (bytes)	[0;2500]
DIFS (µs)	26
SIFS (µs)	10
SlotTime (N_s) (µs)	8
$CWmin$ (integer)	63
$CWmax$ (integer)	1023

Table 2: DCF specification

It is assumed that a node transmits in a slot time randomly chosen with a probability τ.The packet been transmitted experiences a collision with a probability p. These two parameters are the main features of Binary Exponential-Backoff (BEB) algorithm in DCF [21]. Considering m attempts, the probabilities τ and p are given by:

$$\begin{cases} \tau = \dfrac{2}{1 + CW + pCW \sum_{i=0}^{m-1}(2p)^i)} \\ p = 1 - (1-\tau)^{n-1} \end{cases} \quad (5)$$

Where n is the number of nodes. This assumes that at least one of the $(n-1)$ remaining nodes transmits in a given slot time. The probability P_{tr} that there is at least one transmission in the considered slot time is:

$$P_{tr} = 1 - (1-\tau)^n \quad (6)$$

The probability P_s that a transmission occurring on the channel is successful is given by:

$$P_s = \frac{n\tau(1-\tau)^{n-1}}{P_{tr}} \quad (7)$$

During the mean time T_{succ}, the channel is detected busy due to a successful transmission. In addition, during the average time T_{col}, the channel is detected as busy because a collision occurred during the transmission attempt [21]:

$$\begin{cases} T_{succ} = RTS + CTS + Data + ACK + 3SIFS + DIFS \\ T_{col} = RTS + DIFS + SIFS + CTS \end{cases} \quad (8)$$

For reasons of simplification, we have supposed that there is no collision, so p = 0% and therefore a successful transmission from the first attempt (m = 1). This is a reasonable approximation because we are studying a network with a very low number of nodes.
In this case, the delay D_{succ} of a successfully transmitted packet can be obtained from [21]:

$$D_{succ} = L_{slot}\, N_{slot} \quad (9)$$

L_{slot} is the average length of a slot time which and N_{slot}, the average number of time slots for a successful packet transmission.
L_{slot} is expressed as follows:

$$L_{slot} = P_{idle}N_s + P_{succ}T_{succ} + P_{col}T_{col} \quad (10)$$

P_{succ} and P_{col} are respectively expressed as :

$$\begin{cases} P_{succ} = P_{tr}P_s \\ P_{col} = P_{tr} - P_s \end{cases} \quad (11)$$

The probability of having a randomly chosen idle slot P_{idle} is obtained from:

$$P_{idle} = 1 - P_{tr} \quad (12)$$

N_{slot} is expressed as follows:

$$N_{slot} = \frac{(1+CW)(1-2p) + CWp(1-(2p)^m)}{2(1-2p)(1-p)} \qquad (13)$$

In the following, we determine the successful delay D_{succ} defined in (9), using the DCF parameters of table 2.

4 Performance analysis

In order to evaluate performance considering both PHY and MAC layer metrics, we determine the trade-offs between the emitted power and the delay corresponding to a successful packet transmission. For this aim, we first consider the packet error rate (PER) defined by:

$$PER = 1 - (1 - BER)^N \qquad (14)$$

The BER is a PHY layer metric, linked to the optical emitted power. The number of bits N is the packet size, a MAC layer parameter. Thus, PER metric is considered as a cross-layer PHY/MAC metric from which we will be able to discuss on the trade-offs between emitted power and delay of successful transmission.

4.1 Emitted power P_t for a target quality of service

From (3)-(4), we can compute the BER as a function of the SNR according OOK and L-PPM modulations. Using (1), we then determine the value of P_t required to reach a given SNR so BER, according data rate R_b. In this section, we consider the worst DC gain values reported in Table 1 (values in bold) for uplink and downlink. Considering the maximal MPDU size from specifications reported on Table 2 (2500 bytes, so N=2500*8 bits) and a targeted PER of 10^{-3}, this corresponds to a BER of around $5x10^{-8}$. For this BER value, the minimal average emitted power P_t is determined as a function of the data rate and reported in Fig.5 for OOK and 4-PPM modulations.

As expected, for a given performance, increasing the data rate R_b requires increasing the emitted power P_t. In addition, we can note that the required power with OOK modulation is more important than with a 4-PPM for both uplink and downlink configurations. This permits verifying power efficiency of 4-PPM modulation over OOK. For example, for R_b=1Mbps, the required power is 365mW with 4-PPM and 710mW with OOK for the uplink. Another way to interpret this curve is to analyze the data rate for a given transmitted power, which is much more important with 4-PPM than with OOK. For example, for an emitted power of 300mW, the data rate in uplink for OOK is around 180 kbps whereas it is of 670 kbps for 4-PPM, so almost multiplied by a factor 4. In addition, it can be noted that the power required is higher for the downlink than for the uplink. Indeed, the DC gain H_0 considered is lower in downlink than in uplink. This observation has to be taken into account as we use infrared waves. Indeed, emitted power is limited by the eye safety criterion defined in the available standards. For laser equipment, the basic standard is the IEC 60825-1[23], for lamps and LEDs, it is the IEC 62471 [24]. Another important performance indicator depending on the data rate is the transmission delay, as presented in the next section.

4.2 Successful transmission delay for a target quality of service

As described from part 3, the transmission delay depends on data rate and on network parameters. The network is constituted of the four pilots and the AP. Results are reported in Fig.6, as a function of the data rate R_b for network parameter values summarized in Table 3 and for the two extreme contention window values CW equals to 63 and 1023. We first observe that as expected, the delay D_{succ} decreases when R_b increases. For a data rate of 2Mbps, it reaches values around 45ms, respectively. 55ms, for $CWmin$, respectively. $CWmax$. In this case, the contention window variation has an impact of around 18% on the delay. For lower data rates, the delay increases, but the relative variation is lower. For example, for $R_b = 0.6Mbps$, the delay varies from 155ms to 178ms according CW. This corresponds to 13% of increase between the minimal CW value and the maximal one. To reduce the delay, the data rate can be increased, but the value of the CW window has a slightly larger effect. In addition, the increase in data rate is limited by the power value as indicated in part 4.1. Therefore, we have compromises between power and delay. To illustrate the trade-offs between emitted power and successful transmission delay, we consider in this analysis 4-PPM modulation with an emitted power of P_t=300mW. From Fig.5, the maximal achievable data rates for a targeted PER of 10^{-3} in downlink, respectively uplink, are 290 kbps, respectively 670 kbps. Considering these two data rates, we have reported in Table 4 the delay obtained with maximal MPDU size of 2500 bytes, for the two extreme values of CW. We can observe that the minimal reachable delay in this case is 138ms. We analyse in the following the impact of PER value and higher order L of PPM modulation on the emitted power, thus on the delay.

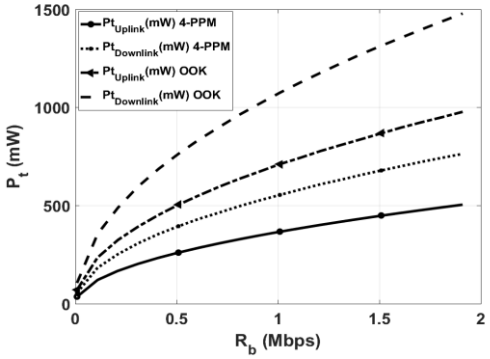

Figure 5: P_t according R_b PER= 10^{-3}, MPDU = 2500 bytes

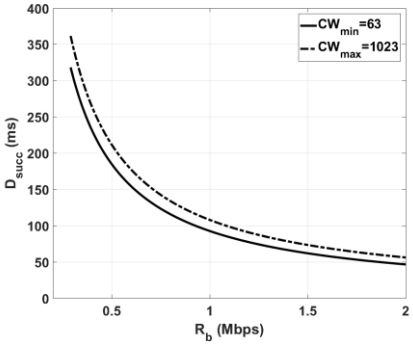

Fig.6 D_{succ} according R_b. MPDU=2500 bytes, CW_{min}=63 and CW_{max}=1023

Attribut	Values
n	5
m	1
p	0%

Table 3: Network parameters

	Date rate	CW_{min}=63	CW_{max}=1023
MPDU 2500 bytes	290 kbps	318 ms	362 ms
	670 kbps	138 ms	159 ms

Table 4: Delay D_{succ}, 4-PPM modulation, P_t=300mW

4.3 Impact of targeted PER and higher order modulation

As an example, we focus here on the uplink. We have reported in Fig.7 the minimal emitted power required to reach different targeted PER with 4-PPM modulation and with 16-PPM for targeted PER of 10^{-3}. As expected, we can observe that the power required with a given data rate is decreased when the targeted PER is higher, and even more when using a 16-PPM instead of the 4-PPM. For example, for the data rate of 670 kbps (corresponding to a PER of 10^{-3} with P_t=300mW) we can note that emitted power is equal to 320mW for PER=10^{-4}, reduced to 250mW for PER=10^{-2} and even to 110mW for a 16-PPM modulation with PER=10^{-3}. In addition, we can determine from Fig. 7 for each configuration the corresponding maximal reachable data rate and then by using Fig.6, the corresponding delay for a given emitted power. Values are reported in Table 5 for P_t=300mW. For the 16-PPM configuration, it is not possible to extract results from Fig. 7 due to the range of the axis, but the analysis was done following the same process. We can observe from values in Table 5 that reducing the constraint on targeted PER by one decade (PER=10^{-2}) permits lowering the delay by approximately 30%. Furthermore, changing the order of the modulation to 16-PPM has a much more significant impact (delay reducing by 85%), but at the cost of an implementation complexity increase and potential Inter Symbol Interference (ISI) due to a greater required bandwidth.

5 Conclusions

In this article, we have studied a network composed of four audio headsets connected in optical wireless and an access point to the cockpit ceiling of an Airbus A350. The main objective was to study the trade-offs as a function of the data rate and linked to the physical channel parameters, in particular the transmission power, and those resulting from the channel access method based on DCF with RTS / CTS. We first studied the modelling of the channels for the uplink and downlink between the headsets and the access point. This contribution was based on the advanced cockpit simulation from a 3D geometric model of the cockpit. In addition, the presence of the pilots and their movements was taken into account. Simulation of the channel by ray tracing associated with a Monte-Carlo method allowed determining the gain values of the channel in a worse case but with 100% reliability in uplink and downlink. The results show that the worst case corresponds to the position of the rear co-pilot. Based on these results, we then performed a combined analysis of the transmitted power and the delay for successful communication. The minimum optical power necessary for a given performance has been evaluated for conventional OWC modulation schemes (OOK and PPM) as a function of the data rate. Likewise, we have studied the delay values for successful communication in the network for the studied protocol. The approach has highlighted the trade-offs between power and delay linked to maximal achievable data rate for a given performance. Finally, we have shown that increasing the order of the modulation is the most effective way to reduce the delay but at the cost of an implementation complexity and potential ISI. When a very low delay is required, adding diversity on the headset can be investigated as an alternative.

	Targeted PER	Date rate	$CWmin$ =63	$CWmax$ =1023
4-PPM	PER=10^{-4}	590 kbps	**157 ms**	**180 ms**
	PER=10^{-3}	670 kbps	**138 ms**	**159 ms**
	PER=10^{-2}	970 kbps	**96 ms**	**111 ms**
16-PPM	PER=10^{-3}	5 Mbps	**19 ms**	**25.2 ms**

Table 5: Delay D_{succ}, P_t=300mW for different target PER and MDPU = 2500 bytes

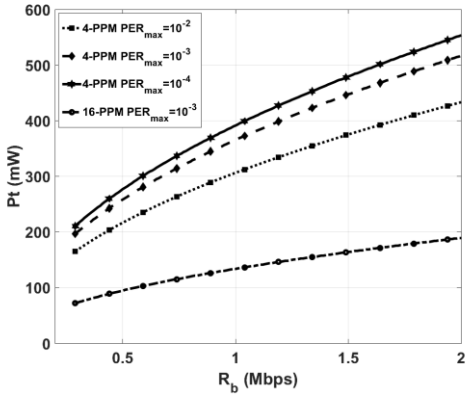

Figure 7: Emitted power P_t as a function of R_b for different PER with 4-PPM and for PER=10^{-3} with 16-PPM.

References

[1] Dinh-Khanh Dang, A. Mifdaoui and T. Gayraud, "Fly-By-Wireless for next generation aircraft: Challenges and potential solutions," 2012 IFIP Wireless Days, Dublin, 2012, pp. 1-8. doi: 10.1109/WD.2012.6402820

[2] Y. Zou, J. Zhu, X. Wang, and L. Hanzo, "A survey on wireless security: Technical challenges, recent advances, and future trends" Proc. IEEE, vol. 104, no. 9, pp. 1727–1765, Sep. 2016

[3] S. Arnon, J. Barry, G. Karagiannidis, R. Schober, and M. Uysal, editors. *Advanced Optical Wireless Communication Systems*. Cambridge University Press, 2012.

[4] [S. Arnon, editor. *Visible Light Communication*. Cambridge University Press, 1st edition, 2015.

[5] [S. Dimitrov and H. Haas, editors. *Principles of LED Light Communications Towards Networked Li-Fi*. Cambridge University Press, 1st edition, 2015.

[6] Z. Ghassemlooy, L.N. Alves, S. Zvanovec, and M-A Khalighi, editors. *Visible Light Communications: Theory and Applications*. CRC Press, 1st edition, 2017.

[7] N. Schmitt. "Wireless optical NLOS Communication in Aircraft Cabin for In-flight Entertainment" In Proceedings of ESA 1st Optical Wireless Onboard Communications Workshop, September 2004.

[8] S. Dimitrov, H. Haas, M. Cappitelli, and M. Olbert."On the throughput of an OFDM-based cellular optical wireless system for an aircraft cabin". In Proceedings of the 5th European Conference on Antennas and Propagation (EUCAP), pages 3089–3093, Roma, May 2011.

[9] C. Vassilopoulos, D. Marinos, A. C. Boucouvalas, N. P. Schmitt, Th.Pistner, and C. Aidinis. "Diffuse wireless optical link for aircraft intra-cabin passenger communication". In Proceedings of the fifth International Symposium on Communication Systems Networks and Digital Signal Processing C.3: Optical Wireless Systems, pages 625–628, July 2006.

[10] D. Marinos, F. Leonidas, N. Vlissidis, C. Giovanis, G. Pagiatakis,C. Aidinis, C. Vassilopoulos, T. Pistner, N. Schmitt, and J. Klaue. "Medical and safety monitoring system over an in-cabin optical wireless network". International Journal of Electronics, 98(2):223–233, feb 2011

[11] S. Dimitrov, R. Mesleh, H. Haas, M. Cappitelli, M. Olbert and E. Bassow, "Path Loss Simulation of an Infrared Optical Wireless System for Aircrafts", GLOBECOM 2009 - 2009 IEEE Global Telecommunications Conference, Honolulu, HI, 2009, pp. 1-6

[12] S.Jpumessi-Demeffo, S.Sahuguede, D.Sauveron, A.Julien-Vergonjanne et al "A Link Reliability Study of Optical Wireless Headset inside Aircraft Cockpit" 2019 Global LIFI Congress (GLC), Paris, France, 2019, pp. 1-6.doi: 10.1109/GLC.2019.8864135

[13] Z. Ghassemlooy, W. Popoola, and S. Rajbhandari, *Optical wireless communications: system and channel modelling with Matlab®*. CRC Press, 2012

[14] A. Mahdiraji and E. Zahedi, "Comparison of Selected Digital Modulation Schemes (OOK, PPM and DPIM) for Wireless Optical Communications," in In the Proceeding of the 4th Student Conference on Research and Development (SCOReD 06), Jun. 27–28, 2006, pp. 5–10.

[15] H. Haas, L. Yin, Y. Wang, and C. Chen, "What is LiFi?" J. Lightw. Technol., vol. 34, no. 6, pp. 1533–1544, Mar. 2016.

[16] IEEE, «Part 11: Wireless LAN medium access control (MAC) and physical layer (PHY) specifications,» pp. 1489-1503, 2012.

[17] A. Behlouli, P. Combeau, and L. Aveneau. "MCMC Methods for Realistic Indoor Wireless Optical Channels Simulation." IEEE/OSA Journal of Lightwave Technology, 35(9):1575–1587, May 2017

[18] Blender. https://www.blender.org.

[19] A.J.C. Moreira, R.T. Valadas, and A.M. de Oliveira Duarte. "Characterization and modelling of artificial light interference in optical wireless communication systems". In Proceedings of 6th International Symposium on Personal, Indoor and Mobile Radio Communications, pages 326–331. IEEE, September 1995

[20] M. Dehghani Soltani, X. Wu, M. Safari and H. Haas, "Bidirectional User Throughput Maximization Based on Feedback Reduction in LiFi Networks," in IEEE Transactions on Communications, vol. 66, no. 7, pp. 3172-3186, July 2018.doi: 10.1109/TCOMM.2018.2809435

[21] G. Bianchi, "Performance analysis of the IEEE 802.11 distributed coordination function," in IEEE Journal on Selected Areas in Communications, vol. 18, no. 3, pp. 535-547, March 2000.doi: 10.1109/49.840210

[22] Alabady, S.A., Salleh, M.F.M. & Hasib, A. Throughput and Delay Analysis of IEEE 802.11 DCF in the Presence of Hidden Nodes for Multi-hop Wireless Networks. Wireless Pers Commun 79, 907–927 (2014). https://doi.org/10.1007/s11277-014-1894-9

[23] 'IEC 60825-1.2007, Safety of laser products — Part1 Equipment classification and requirement'.

[24] 'IEC 62471 (2006) Photobiological safety of lamps and lamp systems (identical with CIE S009)'.